MATHEMATICAL ENGINEERING
TECHNICAL REPORTS

Improvement of the Scaled Corrector Method for Bifurcation Analysis Using Symmetry-Exploiting Block-Diagonalization

Kiyohiro IKEDA, Kazuo MUROTA,
Akito YANAGIMOTO, and
Hirohisa NOGUCHI

METR 2006–02 January 2006

DEPARTMENT OF MATHEMATICAL INFORMATICS
GRADUATE SCHOOL OF INFORMATION SCIENCE AND TECHNOLOGY
THE UNIVERSITY OF TOKYO
BUNKYO-KU, TOKYO 113-8656, JAPAN

WWW page: http://www.i.u-tokyo.ac.jp/mi/mi-e.htm

Improvement of the scaled corrector method for bifurcation analysis using symmetry-exploiting block-diagonalization

Kiyohiro IKEDA[1]
Department of Civil Engineering, Tohoku University, Aoba, Sendai 980-8579, Japan

Kazuo MUROTA
Department of Mathematical Informatics, Graduate School of Information Science and Technology, University of Tokyo, Tokyo 113-8656, Japan

Akito YANAGIMOTO
Department of Civil Engineering, Tohoku University, Aoba, Sendai 980-8579, Japan

Hirohisa NOGUCHI
Department of System Design Engineering, Keio University, Yokohama 223-8522, Japan

January 8, 2006

[1]Corresponding author: ikeda@civil.tohoku.ac.jp; tel:81-22-795-7416; fax:81-22-795-7418.

ABSTRACT: In the nonlinear bifurcation analysis for large scaled structures, the standard eigenanalysis of the tangent stiffness matrix yields important information, but, at the same time, demands a large amount of computational cost. The scaled corrector method was developed as a numerically efficient, eigenanalysis-free, bifurcation-analysis strategy, which exploits byproducts of the numerical iteration for path tracing. This method, however, has a problem in its accuracy, especially when eigenvalues are nearly or exactly coincidental. As a remedy for this, we propose a new bifurcation analysis method through the implementation of bifurcation mechanism of a symmetric structure into the scaled corrector method. The bifurcation mode is accurately approximated by decomposing a scaled corrector vector into a number of vectors by means of block diagonalization method in group-theoretic bifurcation theory and, in turn, by choosing the predominant one among these vectors. In order to demonstrate the usefulness of this method, it is applied to the bifurcation analysis of reticulated regular-hexagonal truss domes to compute accurately the locations of double bifurcation points and nearly coincidental bifurcation points, and associated bifurcation modes.

Keywords: bifurcation analysis, block diagonalization, dihedral group, scaled corrector, symmetric structures

1 Introduction

The finite-element nonlinear bifurcation analysis of structures has drawn keen interest, and a number of numerical procedures have been developed for bifurcation point detection and branch-switching. It is common to detect bifurcation points via the tracing of the equilibrium paths (Riks [25, 26], Eriksson [3], Choong and Hangai [1], Fujii and Ramm [6]). The direct method does not necessitate the path-following analysis in the computation of the stability point via the construction of an extended system (Wriggers et al. [33], Wriggers and Simo [34]); the pinpointing of the stability point is possible by solving the extended system (Fujii and Ramm [6]; Fujii et al. [4]).

In the nonlinear bifurcation analysis for large scaled structures, the standard eigenanalysis of the tangent stiffness matrix yields important information, but, at the same time, demands a large amount of computation, despite the study on the solution methods of the finite element eigenanalysis (Sehmi [29]; Papadrakakis [24]). Eigenanalysis-free bifurcation-analysis strategies, which exploit byproducts in the numerical iteration to obtain equilibrium points, were developed (Noguchi and Hisada [23], Fujii and Noguchi [5], Noguchi and Fujii [22]). A scaled corrector, which is a normalized correction vector in the Newton–Raphson iteration in the corrector step, was found to simulate well the critical eigenvector in the vicinity of a critical point (Noguchi and Hisada [23]); it achieved numerical efficiency but, at the same time, encountered the following difficulties:

- Nearly coincidental bifurcation points cannot be separated.
- Simple and double bifurcation points cannot be distinguished.
- For a double bifurcation point, which has two critical eigenvectors, only a single critical eigenvector can be obtained.

Structures with axisymmetry or regular-polygonal symmetry, such as reticulated domes and cylindrical shells, are known to have double bifurcation points. The bifurcation of these structures was studied as a bifurcation problem of dihedral-group symmetry by group-theoretic bifurcation theory (Healey [10], Ikeda et al. [16], Gatermann [7], Gatermann and Werner [8], Wohlever and Healey [32], Wohlever [31], Ikeda and Murota [15]). This theory was implemented into the framework of FEM (Zingoni [35], Lin [18]). Block-diagonalization method was employed to exploit symmetry and to reduce the computational cost involved (Healey [10], Zloković [36], Dinkevich [2], Healey and Treacy [11], Ikeda and Murota [14], Murota and Ikeda [21], Ikeda et al. [12]), and to classify vibration modes (Mohan and Pratap [19, 20]). This method was employed to investigate the possible occurrence of bifurcations in materials (Ikeda et al. [13, 17]).

A new bifurcation analysis procedure is proposed in this paper by incorporating the bifurcation mechanism of symmetric structures into the scaled corrector method. The bifurcation mode is accurately approximated by decomposing a scaled corrector vector

into a number of vectors on the basis of the symmetry of the structure and, in turn, by choosing the predominant one. The usefulness of this technique is demonstrated through its application to the bifurcation analysis of reticulated regular-hexagonal truss domes to extract bifurcation modes, and to accurately search for the locations of bifurcation points.

2 Group-theoretic bifurcation theory

We introduce in this section a brief account of group-theoretic bifurcation theory as a summary of Ikeda and Murota [15]. More mathematical issues can be found, e.g., in Sattinger [28] and Golubitsky et al. [9].

2.1 Group equivariance

Consider a sufficiently smooth nonlinear governing equation of a discretized system

$$\mathbf{F}(\mathbf{u}, f) = \mathbf{0}, \tag{1}$$

where $\mathbf{F} = (F_1, F_2, \ldots, F_n)^{\mathrm{T}}$ is an n-dimensional nonlinear function vector, $\mathbf{u} = (u_1, u_2, \ldots, u_n)^{\mathrm{T}}$ is an n-dimensional (nodal displacement) vector, and f is a (loading) parameter. In this paper we assume that $\mathbf{F}$ is derived from a potential function, which implies that the tangent stiffness matrix $K = \partial\mathbf{F}/\partial\mathbf{u}$ is a symmetric matrix.

The symmetry of the nonlinear governing equation (1) is expressed by the equivariance to a group G, namely,

$$T(g)\mathbf{F}(\mathbf{u}, f) = \mathbf{F}(T(g)\mathbf{u}, f), \qquad \text{for } g \in G, \tag{2}$$

where an element g of G represents a geometrical transformation, and $T(g)$ is an orthogonal $n \times n$ representation matrix expressing the influence of g on the vectors $\mathbf{F}$ and $\mathbf{u}$. The pre-bifurcation solutions $(\mathbf{u}, f)$ are assumed to be G-invariant in the sense that

$$T(g)\mathbf{u} = \mathbf{u}, \qquad \text{for } g \in G, \tag{3}$$

while a bifurcated solution has a reduced symmetry labeled by a subgroup of G. Hence a recursive occurrence of bifurcation is described by a hierarchy of subgroups[2]

$$G \to G_1 \to G_2 \to \cdots \tag{4}$$

Here $\to$ denotes the occurrence of bifurcation, and G_i $(i = 1, 2, \cdots)$ stand for subgroups of G that label the reduced symmetry of the bifurcated solutions.

2.2 Block diagonalization

Let V be the space of solutions $\mathbf{u}$ of system (1) that is G-equivariant in the sense of (2). According to the theory of group representation, the space V is decomposed uniquely into a direct sum as

$$V = \bigoplus_{\mu \in R(G)} V^{\mu}, \tag{5}$$

[2] Actual forms of (4) for particular groups are given, e.g., in Ikeda et al. [13], Ikeda and Murota [15], Tanaka et al. [30], and Saiki et al. [27].

where V^μ denotes the subspace associated with a (real) irreducible representation[3] μ of G, and $R(G)$ indicates the set of all irreducible representations of G. The decomposition (5) is called the isotypic decomposition.

In accordance with the decomposition (5), we may consider the coordinate transformation

$$\mathbf{u} = \sum_{\mu \in R(\mathrm{G})} H^\mu \mathbf{u}^\mu, \tag{6}$$

where $\mathbf{u}^\mu$ is an independent variable associated with the subspace V^μ, and H^μ is a matrix made up of vectors forming an orthonormal basis of the subspace V^μ. Collecting H^μ for all $\mu \in R(G)$, we define

$$H = (\ldots, H^\mu, \ldots), \tag{7}$$

which is an $n \times n$ orthogonal matrix ($H^{\mathrm{T}} H = I_n$ with the identity matrix I_n of order n). The transformation matrix H is not uniquely determined, but it should be chosen in view of other factors, such as computational cost for the transformation. A natural choice for discrete structures, such as trusses, is suggested in [21].

As a consequence of (2) and (3), the tangent stiffness matrix $K = \partial \mathbf{F}/\partial \mathbf{u}$ commutes with $T(g)$ for all $g \in G$, i.e.,

$$T(g)K = KT(g), \quad \text{for } g \in G. \tag{8}$$

It follows from (8) that the matrix K can be transformed by H in (7) into a block diagonal form:

$$\tilde{K} = H^{\mathrm{T}} K H = \begin{pmatrix} \ddots & & O \\ & \tilde{K}^\mu & \\ O & & \ddots \end{pmatrix}, \tag{9}$$

where $\tilde{K}^\mu = (H^\mu)^{\mathrm{T}} K H^\mu$. Since $\det \tilde{K} = 0$ if and only if $\det \tilde{K}^\mu = 0$ for some μ, the critical points can be classified according to the diagonal block $\tilde{K}^\mu$ that becomes singular. It is noted that, generically, such μ is uniquely determined for a critical point.

[3] An irreducible representation means a representation matrix that does not split into a direct sum of representations of smaller sizes. See, e.g., Ikeda and Murota [15] for this account.

3 Scaled corrector method

The scaled corrector method is briefly reviewed (Noguchi and Hisada [23]).

3.1 Newton iteration

We consider predictor-corrector steps during path-tracing of the governing equation (1). In the corrector step, with the use of the corrector $(\delta\mathbf{u}, \delta f)$, which is expected to reduce the norm $||\mathbf{F}(\mathbf{u}, f)||$, is determined from the Newton equation

$$K\delta\mathbf{u} - \mathbf{p}\delta f = -\mathbf{F}(\mathbf{u}, f), \tag{10}$$

where $\mathbf{p} = -\partial\mathbf{F}/\partial f$. When K is nonsingular, we have

$$\delta\mathbf{u} = K^{-1}(\mathbf{p}\delta f - \mathbf{F}(\mathbf{u}, f)). \tag{11}$$

Consider the eigenvalue problem of the tangent stiffness matrix K:

$$K\boldsymbol{\Phi}_j = \lambda_j\boldsymbol{\Phi}_j, \tag{12}$$

where λ_j and $\boldsymbol{\Phi}_j$ are the eigenvalue and eigenvector of K, respectively; it is assumed that $(\boldsymbol{\Phi}_j)^{\mathrm{T}}\boldsymbol{\Phi}_j = 1$ and $(\boldsymbol{\Phi}_i)^{\mathrm{T}}\boldsymbol{\Phi}_j = 0$ if $i \neq j$. It then follows that

$$\lambda_j = (\boldsymbol{\Phi}_j)^{\mathrm{T}}K\boldsymbol{\Phi}_j. \tag{13}$$

When K is nonsingular, we have

$$K^{-1} = \sum_{j=1}^{n} \frac{1}{\lambda_j}\boldsymbol{\Phi}_j(\boldsymbol{\Phi}_j)^{\mathrm{T}}. \tag{14}$$

3.2 Simple critical point

Suppose that we consider a simple bifurcation point and denote the eigenvalue vanishing at this point by λ_1. In the vicinity of this point, the eigenvalue λ_1 approaches zero, and, in turn, $|1/\lambda_1|$ becomes very large. Then (14) can be approximated as

$$K^{-1} \simeq \frac{1}{\lambda_1}\boldsymbol{\Phi}_1(\boldsymbol{\Phi}_1)^{\mathrm{T}}. \tag{15}$$

With the use of (15) in (11), we obtain

$$\delta\mathbf{u} \simeq [\frac{1}{\lambda_1}(\boldsymbol{\Phi}_1)^{\mathrm{T}}(\mathbf{p}\delta f - \mathbf{F})]\boldsymbol{\Phi}_1, \tag{16}$$

which indicates that the eigenvector $\boldsymbol{\Phi}_1$ for the eigenvalue λ_1 in question can be approximated by the corrector $\delta\mathbf{u}$. Hence by defining the scaled corrector

$$\boldsymbol{\Phi}^{\mathrm{sc}} = \frac{\delta\mathbf{u}}{||\delta\mathbf{u}||} \tag{17}$$

with the corrector $\delta\mathbf{u}$ in (11), we have

$$\mathbf{\Phi}^{\rm sc} \simeq \mathbf{\Phi}_1. \tag{18}$$

Combining this with (13) motivates the definition of a pseudo-eigenvalue $\hat{\lambda}$:

$$\hat{\lambda} = (\mathbf{\Phi}^{\rm sc})^{\rm T} K \mathbf{\Phi}^{\rm sc}. \tag{19}$$

Since $\mathbf{\Phi}^{\rm sc}$ approximates $\mathbf{\Phi}_1$ in the vicinity of the simple critical point, we have

$$\hat{\lambda} \simeq \lambda_1 \simeq 0. \tag{20}$$

In numerical analysis, accordingly, the location of a bifurcation point can be monitored by the vanishing of the value of pseudo-eigenvalue $\hat{\lambda}$.

It is noted that, by a well-known fact in linear algebra, we have

$$\hat{\lambda} \geq \min_j \lambda_j \tag{21}$$

for any vector $\mathbf{\Phi}^{\rm sc}$ of unit length. This means that $\hat{\lambda}$ is an approximation of λ_1 from the above in the most customary case where λ_1 is the smallest eigenvalue and the simple critical point in question is the first critical point on the fundamental path.

3.3 Nearly coincidental critical points

Consider a nearly coincidental critical point with M (≥ 2) eigenvalues, say, λ_1, ..., λ_M, close to 0. In this case, (15) reduces to

$$K^{-1} \simeq \sum_{j=1}^{M} \frac{1}{\lambda_j} \mathbf{\Phi}_j (\mathbf{\Phi}_j)^{\rm T}, \tag{22}$$

and, in turn, (16) becomes

$$\delta\mathbf{u} \simeq \sum_{j=1}^{M} [\frac{1}{\lambda_j} (\mathbf{\Phi}_j)^{\rm T} (\mathbf{p}\delta f - \mathbf{F})] \mathbf{\Phi}_j. \tag{23}$$

Then the scaled corrector and the pseudo-eigenvalue are expressed respectively as

$$\mathbf{\Phi}^{\rm sc} \simeq \sum_{j=1}^{M} c_j \mathbf{\Phi}_j, \tag{24}$$

$$\hat{\lambda} \simeq \sum_{j=1}^{M} (c_j)^2 \lambda_j, \tag{25}$$

with some constants c_j ($j = 1, \ldots, M$). Thus $\mathbf{\Phi}^{\rm sc}$ ceases to simulate accurately $\mathbf{\Phi}_1$ due to the mixing with $\mathbf{\Phi}_j$ ($j = 2, \ldots, M$); $\hat{\lambda}$ also becomes inaccurate.

3.4 Double critical points

Consider a double bifurcation point at which two zero eigenvalues say, λ_1 and λ_2, vanish. For this point, (24) and (25) respectively become

$$\mathbf{\Phi}^{\mathrm{sc}} \simeq c_1\mathbf{\Phi}_1 + c_2\mathbf{\Phi}_2, \tag{26}$$

$$\hat{\lambda} \simeq (c_1)^2\lambda_1 + (c_2)^2\lambda_2. \tag{27}$$

It is possible to search for the location of the double bifurcation point as a point where the pseudo-eigenvalue $\hat{\lambda}$ vanishes. Yet, only a single vector $\mathbf{\Phi}^{\mathrm{sc}}$, which is an approximation to the mixture of $\mathbf{\Phi}_1$ and $\mathbf{\Phi}_2$, can be obtained, while in the tracing of the bifurcated paths the two critical eigenvectors $\mathbf{\Phi}_1$ and $\mathbf{\Phi}_2$ in general need to be employed (cf., Subsection 5.3).

4 Revised scaled corrector method

As we have seen in Section 3, the scaled corrector method has problems at coincidental or nearly coincidental bifurcation points. As a remedy for this, the method is revised through the implementation of the block-diagonalization for symmetric structures presented in Subsection 2.2.

With the use of the decomposition (5) of the solution space, the scaled corrector is expanded into a number of vectors with particular symmetries

$$\mathbf{\Phi}^{\mathrm{sc}} = \sum_{\mu \in R(G)} \mathbf{\Phi}^{\mu}, \tag{28}$$

where $\mathbf{\Phi}^{\mu}$ is a vector in V^{μ} expressed using the matrix H^{μ} in (7) as

$$\mathbf{\Phi}^{\mu} = H^{\mu}(H^{\mu})^{\mathrm{T}}\mathbf{\Phi}^{\mathrm{sc}}. \tag{29}$$

Accordingly, we define the pseudo-eigenvalue for each μ by

$$\hat{\lambda}^{\mu} = (\mathbf{\Phi}^{\mu})^{\mathrm{T}} K \mathbf{\Phi}^{\mu} / (\mathbf{\Phi}^{\mu})^{\mathrm{T}} \mathbf{\Phi}^{\mu}. \tag{30}$$

Then, as a ramification of (21), the relationship

$$\hat{\lambda}^{\mu} \geq \lambda^{\mu}_{\mathrm{min}} \tag{31}$$

is satisfied, where $\lambda^{\mu}_{\mathrm{min}}$ is the smallest eigenvalue of $\tilde{K}^{\mu}$ in (9).

Consider a neighborhood of a critical point and denote by μ^* the irreducible representation associated with this critical point. Then a critical eigenvalue, say λ_1, is an eigenvalue of $\tilde{K}^{\mu^*}$ and we have

$$\hat{\lambda}^{\mu^*} \simeq \lambda_1 \simeq 0. \tag{32}$$

In practice, a particular μ^* need to be identified. A procedure suggested in this paper is:

- compute $\hat{\lambda}^{\mu}$ for all μ by (30) using (17) and (29),
- for each μ, plot $\hat{\lambda}^{\mu}$ against a pertinent displacement component for sufficiently many equilibrium points near the critical point, and
- find a particular $\mu = \mu^*$ for which zero-crossing of the values of $\hat{\lambda}^{\mu}$ is encountered.

In addition to the determining of this location, the type of bifurcation point can be classified in view of the critical eigenvector $\mathbf{\Phi}^{\mu^*}$.

5 Bifurcation of a system with regular-hexagonal symmetry

The bifurcation mechanism of a system with regular-hexagonal symmetry is briefly introduced on the basis of Ikeda and Murota [15]. The revised scaled corrector method for such a system, for which double bifurcation points are encountered generically, is proposed.

5.1 Description of symmetry

The symmetry of a regular hexagon shown in Fig. 1 is expressed by the invariance to the following two kinds of transformations:

- r: counter-clockwise rotation at an angle of $2\pi/6$ about the center of the hexagon, and
- s: reflection with respect to the horizontal axis.

Thus the symmetry of the hexagon is labeled by the dihedral group of degree 6, being defined as

$$\mathrm{D}_6 = \left\{e, r, \cdots, r^5, s, sr \cdots, sr^5\right\}, \tag{33}$$

where e denotes the identity transformation that leaves everything unchanged.

The symmetries of deformed regular hexagons are labeled by the subgroups of D_6,

$$\begin{cases} \{\mathrm{D}_m^k \mid k = 1, \ldots, 6/m;\ m = 1, 2, 3\}, \\ \{\mathrm{C}_m \mid m = 1, 2, 3, 6\}, \end{cases} \tag{34}$$

which are defined as

$$\begin{cases} \mathrm{D}_m^k = \{r^{in/m}, sr^{in/m+k-1} \mid i = 0, 1, \ldots, m-1\}, \\ \mathrm{C}_m = \{r^{in/m} \mid i = 0, 1, \ldots, m-1\}. \end{cases} \tag{35}$$

Here $\mathrm{D}_m^1 = \mathrm{D}_m$, $\mathrm{C}_1 = \{e\}$; C_1 indicates asymmetry. Deformation patterns of the regular hexagon labeled by these subgroups are shown in Fig. 2.

5.2 Irreducible representations of D_6

The group D_6 has four one-dimensional irreducible representations and a pair of two-dimensional irreducible representations, as listed in Table 1. The former corresponds to simple critical points and the latter to double bifurcation points.

We denote the one-dimensional irreducible representations by

$$(+,+),\ (+,-),\ (-,+),\ (-,-), \tag{36}$$

which are defined in terms of the one-dimensional representation matrices as

$$\begin{cases} T^{(+,+)}(r) = \ \ 1, & T^{(+,+)}(s) = \ \ 1 \\ T^{(+,-)}(r) = \ \ 1, & T^{(+,-)}(s) = -1 \\ T^{(-,+)}(r) = -1, & T^{(-,+)}(s) = \ \ 1 \\ T^{(-,-)}(r) = -1, & T^{(-,-)}(s) = -1 \end{cases} \tag{37}$$

where $(-,+)$, for example, indicates the antisymmetry with respect to the rotation r and the symmetry with respect to the reflection s.

The two-dimensional irreducible representations are denoted by (j) for $j = 1, 2$, which are defined respectively by

$$T^{(j)}(r) = \begin{pmatrix} \cos(2\pi j/6) & -\sin(2\pi j/6) \\ \sin(2\pi j/6) & \cos(2\pi j/6) \end{pmatrix}, \quad T^{(j)}(s) = \begin{pmatrix} 1 & 0 \\ 0 & -1 \end{pmatrix}, \quad j = 1, 2. \tag{38}$$

Both of these two-dimensional irreducible representations are absolutely irreducible (irreducible over complex numbers).

In general, the symmetry of an irreducible representation μ of a group G is described by a subgroup $G^\mu = \{g \in G \mid T^\mu(g) = I\}$, which also labels the symmetry of the critical eigenvector that corresponds to μ. In the case of D_6, we have

$$\begin{cases} G^{(+,+)} = \mathrm{D}_n, \quad G^{(+,-)} = \mathrm{C}_n, \quad G^{(-,+)} = \mathrm{D}_{n/2}, \quad G^{(-,-)} = \mathrm{D}^2_{n/2}, \\ G^{(1)} = \mathrm{C}_1, \quad G^{(2)} = \mathrm{C}_2. \end{cases} \tag{39}$$

5.3 Block diagonalization

For a system equivariant to D_6, the isotypic decomposition (5) reads

$$V = V^{(+,+)} \oplus V^{(+,-)} \oplus V^{(-,+)} \oplus V^{(-,-)} \oplus V^{(1)} \oplus V^{(2)}. \tag{40}$$

The transformation matrix (7) for the decomposition (40) is given by

$$H = (H^{(+,+)}, H^{(+,-)}, H^{(-,+)}, H^{(-,-)}, H^{(1)}, H^{(2)}). \tag{41}$$

With the use of the transformation matrix (41), the tangent stiffness matrix K can be put into a block diagonal form (cf., (9)):

$$\begin{aligned} \tilde{K} &= H^{\mathrm{T}} K H \\ &= \begin{pmatrix} \tilde{K}^{(+,+)} & & & & & \\ & \tilde{K}^{(+,-)} & & & O & \\ & & \tilde{K}^{(-,+)} & & & \\ & & & \tilde{K}^{(-,-)} & & \\ & O & & & \tilde{K}^{(1)} & \\ & & & & & \tilde{K}^{(2)} \end{pmatrix} \\ &= \mathrm{diag}\left[\tilde{K}^{(+,+)}, \tilde{K}^{(+,-)}, \tilde{K}^{(-,+)}, \tilde{K}^{(-,-)}, \tilde{K}^{(1)}, \tilde{K}^{(2)}\right], \end{aligned} \tag{42}$$

where $\mathrm{diag}[\cdots]$ means the block-diagonal matrix with the diagonal block entries therein.

The diagonal block $\tilde{K}^{(j)}$ $(j = 1, 2)$ in (42) for a two-dimensional irreducible representation $\mu = (1)$ or (2) splits further into two identical diagonal blocks, say $\hat{K}^{(j)}$ $(j = 1, 2)$, i.e.,

$$\tilde{K}^{(j)} = \begin{pmatrix} \hat{K}^{(j)} & O \\ O & \hat{K}^{(j)} \end{pmatrix}, \quad j = 1, 2, \tag{43}$$

if $H^{(j)}$ $(j = 1, 2)$ is chosen appropriately (cf., Subsection 5.5); this is a consequence of the absolute irreducibility of μ. Denoting such $H^{(j)}$ $(j = 1, 2)$ as

$$H^{(j)} = (H^{(j)1}, H^{(j)2}), \quad j = 1, 2, \tag{44}$$

we have

$$\hat{K}^{(j)} = (H^{(j)1})^{\mathrm{T}} K H^{(j)1} = (H^{(j)2})^{\mathrm{T}} K H^{(j)2}. \tag{45}$$

Thus the block diagonal form (42) enjoys further block structures, namely,

$$\tilde{K} = \mathrm{diag}\left[\tilde{K}^{(+,+)}, \tilde{K}^{(+,-)}, \tilde{K}^{(-,+)}, \tilde{K}^{(-,-)}, \hat{K}^{(1)}, \hat{K}^{(1)}, \hat{K}^{(2)}, \hat{K}^{(2)}\right]. \tag{46}$$

The two independent (critical) eigenvectors at a double bifurcation point can be obtained from the eigenvalue problem of $\hat{K}^{(j)}$ for $j = 1$ or $j = 2$.

5.4 Classification of critical points

At a critical point, one of the blocks in (42) in general becomes singular and the critical point can be classified in view of the associated irreducible representation listed in Table 1. Namely,

- $(+,+)$ corresponds to a limit point of the loading f.
- $(+,-)$, $(-,+)$, and $(-,-)$ are associated with simple bifurcation points with C_6, D_3-, and D_3^2-invariant critical eigenvectors, respectively. The symmetries of the solutions on bifurcated paths are identical with the symmetries of the critical eigenvectors.
- (j) $(j = 1, 2)$ correspond to double bifurcation points with C_1- and C_2-invariant critical eigenvectors, respectively. The symmetries of the solutions on bifurcated paths labeled by D_j^i-symmetries $(i = 1, \ldots, 6/j)$ are different from the symmetries of the critical eigenvectors labeled by C_j.

5.5 Construction of transformation matrix

A systematic way to construct the transformation matrix H, presented in Murota and Ikeda [21] with reference to the concept of orbit, is described.

The orbit of a nodal point, say, q is defined to be the set of points obtained from q by transformations by the elements g of group G, namely,

$$\{g \cdot q \mid g \in G\}. \tag{47}$$

As shown in Fig. 4, D_6-invariant set of nodal points can be decomposed into the following four types of orbits:

- orbit of type 0 consists of the center node,

- orbit of type 1V consists of six nodes of regular hexagonal shape,
- orbit of type 1M consists of six nodes of regular hexagonal shape in a different direction than 1V, and
- orbit of type 2 consists of a dozen of D_6-invariant nodes.

The column vectors of the transformation matrix H associated with the orbits of types 0, 1V, and 1M are shown in Fig. 5, in which the arrows denote in plane deformations and numerals denote out-of-plane deformations. Note that the orbit of type 2, which is not employed in this paper, is omitted in this figure.

5.6 Implementation into the revised scaled corrector method

The bifurcation mechanism of D_n-invariant system is implemented into the framework of the revised scaled corrector method.

5.6.1 Simple bifurcation point

For a simple bifurcation point, for which μ^* is one-dimensional,

$$\mathbf{\Phi}^{\mu^*} \simeq \mathbf{\Phi}_1 \tag{48}$$

holds in its neighborhood for some μ^*. The critical bifurcation mode, therefore, can be approximated by the scaled corrector $\mathbf{\Phi}^{\mu^*}$, as is also the case with the scaled corrector method.

5.6.2 Double bifurcation point

For a double bifurcation point with two critical eigenvalues, corresponding to a two-dimensional irreducible representation $\mu = (1)$ or $\mu = (2)$, the revised method presented in Section 4 can further be refined. In view of the block structures (43) and (44), split the eigenvector $\mathbf{\Phi}^{(j)}$ for $j = 1$ and $j = 2$ into two independent eigenvectors:

$$\mathbf{\Phi}^{(j)} = \mathbf{\Phi}^{(j)1} + \mathbf{\Phi}^{(j)2}, \quad j = 1, 2, \tag{49}$$

where

$$\mathbf{\Phi}^{(j)1} = H^{(j)1}(H^{(j)1})^{\mathrm{T}}\mathbf{\Phi}^{\mathrm{sc}}, \quad \mathbf{\Phi}^{(j)2} = H^{(j)2}(H^{(j)2})^{\mathrm{T}}\mathbf{\Phi}^{\mathrm{sc}}, \quad j = 1, 2. \tag{50}$$

It turns out to be convenient to choose this decomposition such that $\mathbf{\Phi}^{(j)1}$ is D_j^1-invariant ($j = 1, 2$). Then for $\mu = (1)$ or (2) the definition of the pseudo-eigenvalue (30) may be replaced, with a slight abuse of notation, with

$$\hat{\lambda}^{\mu} = (\mathbf{\Phi}^{(j)i})^{\mathrm{T}} K \mathbf{\Phi}^{(j)i} / (\mathbf{\Phi}^{(j)i})^{\mathrm{T}} \mathbf{\Phi}^{(j)i}, \quad j = 1, 2;\ i = 1, 2. \tag{51}$$

This means that for each μ we have a pair of pseudo-eigenvalues distinguished by $i = 1, 2$.

The two independent eigenvectors $\mathbf{\Phi}^{(j)1}$ and $\mathbf{\Phi}^{(j)2}$ obtained herein is useful in the tracing of bifurcated paths. As was made clear in [15, 21], the bifurcated paths at the double bifurcation point associated with $\mu = (1)$ are to be found in the directions:

$$\begin{cases} \pm\mathbf{\Phi}^{(1)1}, & \mathrm{D}_1(=\mathrm{D}_1^1)\text{-invariant}, \\ \pm T(r)\mathbf{\Phi}^{(1)1}, & \mathrm{D}_1^3\text{-invariant}, \\ \pm T(r^2)\mathbf{\Phi}^{(1)1}, & \mathrm{D}_1^5\text{-invariant}, \\ \pm\mathbf{\Phi}^{(1)2}, & \mathrm{D}_1^4\text{-invariant}, \\ \pm T(r)\mathbf{\Phi}^{(1)2}, & \mathrm{D}_1^6\text{-invariant}, \\ \pm T(r^2)\mathbf{\Phi}^{(1)2}, & \mathrm{D}_1^2\text{-invariant}. \end{cases} \tag{52}$$

The bifurcated paths associated with $\mu = (2)$ are to be found in the directions:

$$\begin{cases} \pm\mathbf{\Phi}^{(2)1}, & \mathrm{D}_2(=\mathrm{D}_2^1)\text{-invariant}, \\ \pm T(r^2)\mathbf{\Phi}^{(2)1}, & \mathrm{D}_2^2\text{-invariant}, \\ \pm T(r^4)\mathbf{\Phi}^{(2)1}, & \mathrm{D}_2^3\text{-invariant}. \end{cases} \tag{53}$$

Fig. 3 illustrates schematically these directions.

Table 1: Classification of critical points of D_6-invariant system

Multiplicity M	Irreducible representations μ	Types of critical points	Symmetry groups	
			Eigenvector	Bifurcated paths
1	$(+,+)$	Limit point of f	D_6	No bifurcation
1	$(+,-)$	Simple bifurcation	C_6	C_6
	$(-,+)$		D_3	D_3
	$(-,-)$		D_3^2	D_3^2
2	(j) $(j=1,2)$	Double bifurcation	C_j	D_j^i $(i=1,\ldots,6/j)$

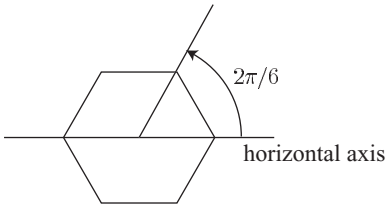

Figure 1: A regular hexagon

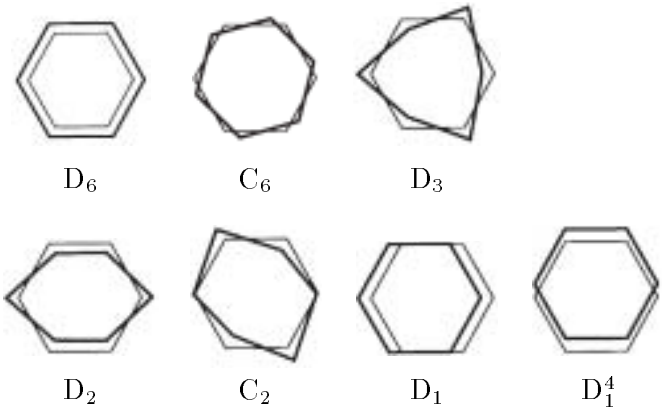

Figure 2: Deformation patterns of the regular hexagon

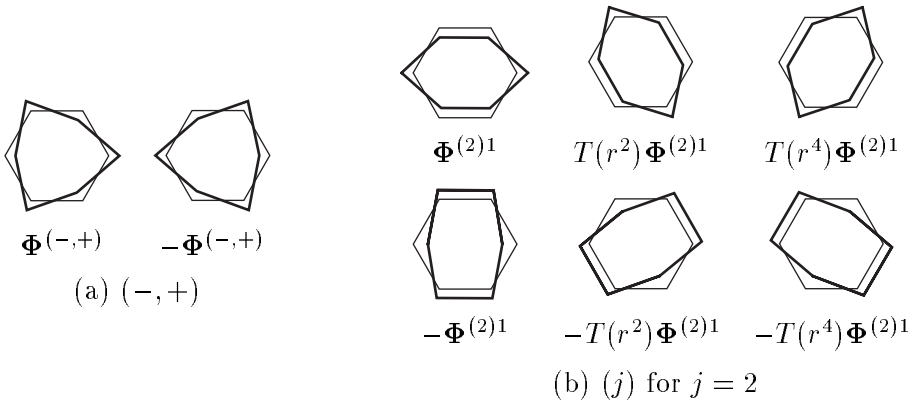

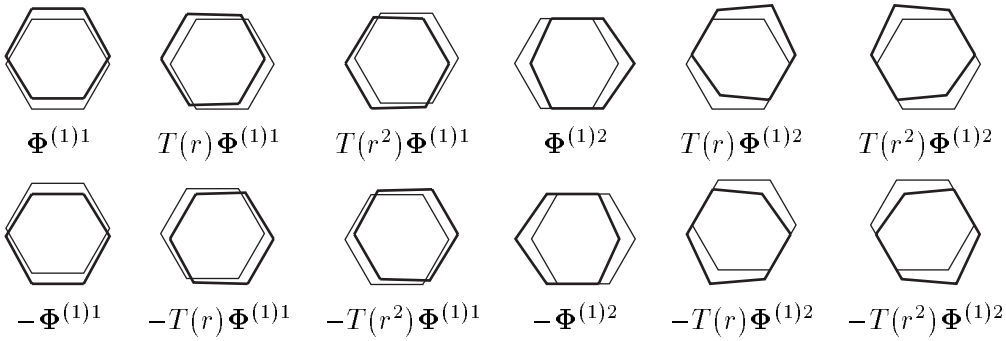

Figure 3: Critical eigenvectors directed towards bifurcated paths

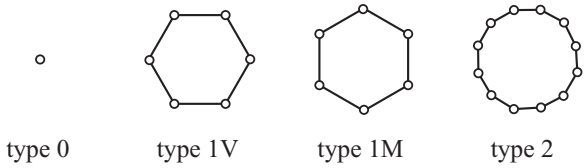

Figure 4: Four types of orbits

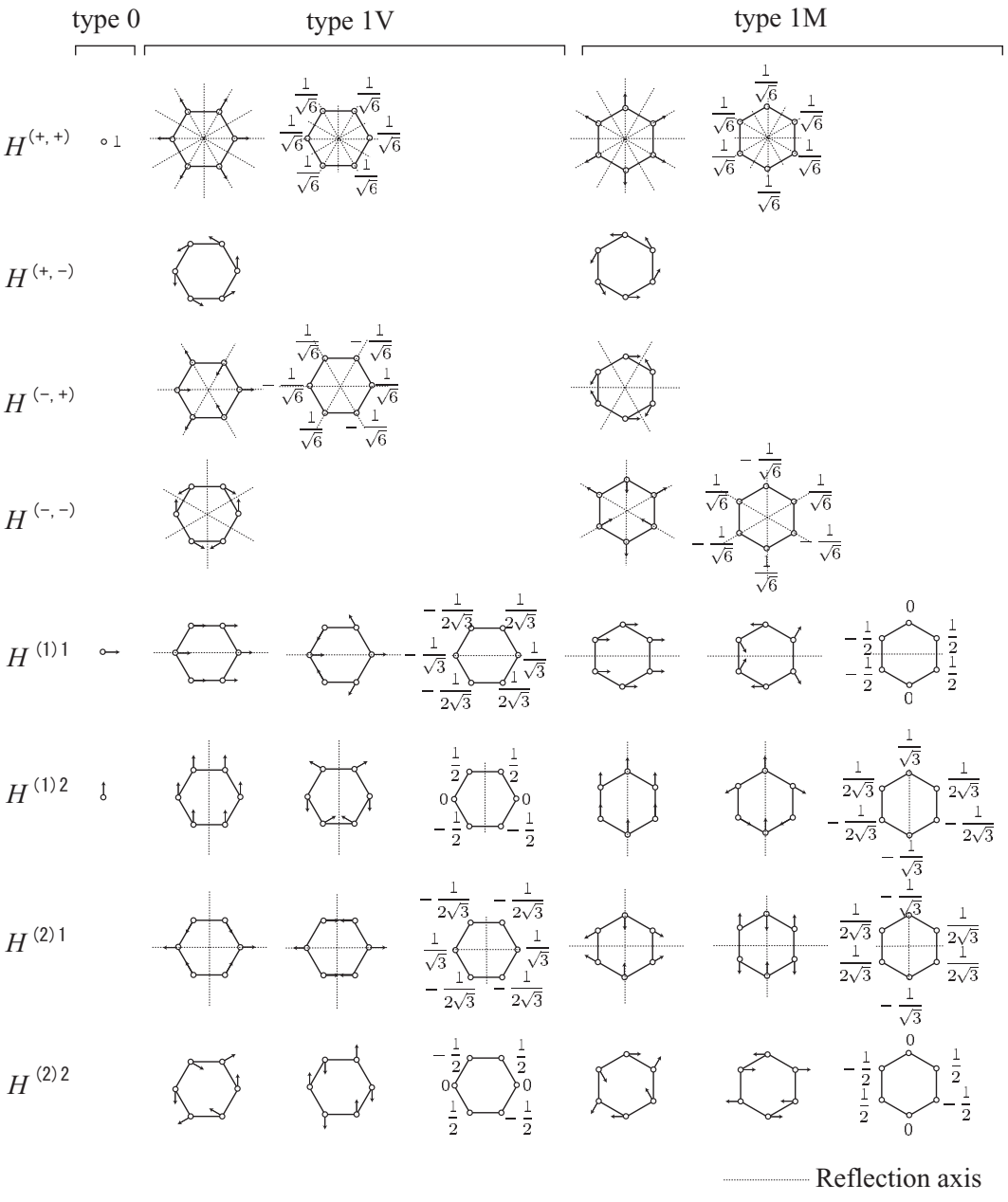

Figure 5: Column vectors of H for the orbits of types 0, 1V, and 1M (the arrows denote in-plane deformation patterns, and the numerals denote out-of-plane deformation patterns)

6 Hangai truss dome

The Hangai truss dome shown in Fig. 6(a) serves as a simple example of D_6-invariant structure; the governing equation of this dome enjoys D_6-equivariance.

Finite displacement elastic bifurcation analysis was conducted to obtain the curves of load versus displacement shown in Fig. 6(b); all members of the dome are assumed to have the same cross section A and the same modulus of elasticity E; we set $EA = 1$ for normalization; the vertical load of $0.2f$ was applied to the center node and the vertical loads of $0.4f$ to the regular hexagonal nodes surrounding the center node.

On the fundamental path with D_6-invariant deformation of this truss dome, there are four critical points:

- bifurcation point A with D_3-invariant bifurcated path,
- bifurcation point B with D_2^i-invariant $(i = 1, 2, 3)$ bifurcated paths,
- bifurcation point C with D_1^i-invariant $(i = 1, \ldots, 6)$ bifurcated paths, and
- limit point D.

See (33) and (35) for the definition of the groups.

6.1 Block diagonalization

The block diagonalization of the tangent stiffness matrix K of the Hangai dome is conducted.

On the fundamental path, K is of the form of

$$K = \begin{bmatrix}
\times & 0 & 0 & \times & 0 & \times & \times & \times & \times & \times & \times & \times & \times & 0 & \times & \times & \times & \times & \times & \times & \times \\
0 & \times & 0 & 0 & \times & 0 & \times & \times & \times & \times & \times & \times & 0 & \times & 0 & \times & \times & \times & \times & \times & \times \\
0 & 0 & \times & \times & 0 & \times & \times & \times & \times & \times & \times & \times & \times & 0 & \times & \times & \times & \times & \times & \times & \times \\
\times & 0 & \times & \times & 0 & \times & \times & \times & 0 & 0 & 0 & 0 & 0 & 0 & 0 & 0 & 0 & 0 & \times & \times & 0 \\
0 & \times & 0 & 0 & \times & 0 & \times & \times & 0 & 0 & 0 & 0 & 0 & 0 & 0 & 0 & 0 & 0 & \times & \times & 0 \\
\times & 0 & \times & \times & 0 & \times & 0 & 0 & \times & 0 & 0 & 0 & 0 & 0 & 0 & 0 & 0 & 0 & 0 & 0 & \times \\
\times & \times & \times & \times & \times & 0 & \times & \times & \times & \times & 0 & 0 & 0 & 0 & 0 & 0 & 0 & 0 & 0 & 0 & 0 \\
\times & \times & \times & \times & \times & 0 & \times & \times & \times & 0 & \times & 0 & 0 & 0 & 0 & 0 & 0 & 0 & 0 & 0 & 0 \\
\times & \times & \times & 0 & 0 & \times & \times & \times & \times & 0 & 0 & \times & 0 & 0 & 0 & 0 & 0 & 0 & 0 & 0 & 0 \\
\times & \times & \times & 0 & 0 & 0 & \times & 0 & 0 & \times & \times & \times & \times & \times & 0 & 0 & 0 & 0 & 0 & 0 & 0 \\
\times & \times & \times & 0 & 0 & 0 & 0 & \times & 0 & 0 & \times & \times & \times & \times & 0 & 0 & 0 & 0 & 0 & 0 & 0 \\
\times & \times & \times & 0 & 0 & 0 & 0 & 0 & \times & \times & \times & \times & 0 & 0 & \times & 0 & 0 & 0 & 0 & 0 & 0 \\
\times & 0 & \times & 0 & 0 & 0 & 0 & 0 & 0 & \times & \times & 0 & \times & 0 & \times & \times & \times & 0 & 0 & 0 & 0 \\
0 & \times & 0 & 0 & 0 & 0 & 0 & 0 & 0 & \times & \times & 0 & 0 & \times & 0 & \times & \times & 0 & 0 & 0 & 0 \\
\times & 0 & \times & 0 & 0 & 0 & 0 & 0 & 0 & 0 & 0 & \times & \times & 0 & \times & 0 & 0 & \times & 0 & 0 & 0 \\
\times & \times & \times & 0 & 0 & 0 & 0 & 0 & 0 & 0 & 0 & 0 & \times & \times & 0 & \times & \times & \times & \times & 0 & 0 \\
\times & \times & \times & 0 & 0 & 0 & 0 & 0 & 0 & 0 & 0 & 0 & \times & \times & 0 & \times & \times & \times & 0 & \times & 0 \\
\times & \times & \times & 0 & 0 & 0 & 0 & 0 & 0 & 0 & 0 & 0 & 0 & 0 & \times & \times & \times & \times & 0 & 0 & \times \\
\times & \times & \times & \times & \times & 0 & 0 & 0 & 0 & 0 & 0 & 0 & 0 & 0 & 0 & \times & 0 & 0 & \times & \times & \times \\
\times & \times & \times & \times & \times & 0 & 0 & 0 & 0 & 0 & 0 & 0 & 0 & 0 & 0 & \times & 0 & \times & \times & \times & \times \\
\times & \times & \times & 0 & 0 & \times & 0 & 0 & 0 & 0 & 0 & 0 & 0 & 0 & 0 & 0 & \times & \times & \times & \times & \times
\end{bmatrix}, \tag{54}$$

where $\times$ means nonzero entries.

The free nodes of the Hangai truss dome, shown in Fig. 6(a), are decomposed into two orbits: the orbit of type 0 for the center node and the orbit of type 1V for the hexagonal nodes surrounding the center node. The transformation matrix H for this case is to be obtained through the assemblage of the column vectors for these two orbits shown in

Fig. 5. With the use of this transformation matrix H in (46), the tangent stiffness matrix K can be put into a block diagonal form

$$\tilde{K} = H^{\mathrm{T}} K H = \mathrm{diag}\left[\tilde{K}^{(+,+)}, \tilde{K}^{(+,-)}, \tilde{K}^{(-,+)}, \tilde{K}^{(-,-)}, \hat{K}^{(1)}, \hat{K}^{(1)}, \hat{K}^{(2)}, \hat{K}^{(2)}\right]$$

$$= \left[\begin{array}{ccccccccccccccccccccc}
\times & \times & \times & 0 & 0 & 0 & 0 & 0 & 0 & 0 & 0 & 0 & 0 & 0 & 0 & 0 & 0 & 0 & 0 & 0 & 0 \\
\times & \times & \times & 0 & 0 & 0 & 0 & 0 & 0 & 0 & 0 & 0 & 0 & 0 & 0 & 0 & 0 & 0 & 0 & 0 & 0 \\
\times & \times & \times & 0 & 0 & 0 & 0 & 0 & 0 & 0 & 0 & 0 & 0 & 0 & 0 & 0 & 0 & 0 & 0 & 0 & 0 \\
0 & 0 & 0 & \times & 0 & 0 & 0 & 0 & 0 & 0 & 0 & 0 & 0 & 0 & 0 & 0 & 0 & 0 & 0 & 0 & 0 \\
0 & 0 & 0 & 0 & \times & \times & 0 & 0 & 0 & 0 & 0 & 0 & 0 & 0 & 0 & 0 & 0 & 0 & 0 & 0 & 0 \\
0 & 0 & 0 & 0 & \times & \times & 0 & 0 & 0 & 0 & 0 & 0 & 0 & 0 & 0 & 0 & 0 & 0 & 0 & 0 & 0 \\
0 & 0 & 0 & 0 & 0 & 0 & \times & 0 & 0 & 0 & 0 & 0 & 0 & 0 & 0 & 0 & 0 & 0 & 0 & 0 & 0 \\
0 & 0 & 0 & 0 & 0 & 0 & 0 & \times & \times & \times & 0 & 0 & 0 & 0 & 0 & 0 & 0 & 0 & 0 & 0 & 0 \\
0 & 0 & 0 & 0 & 0 & 0 & 0 & \times & \times & \times & 0 & 0 & 0 & 0 & 0 & 0 & 0 & 0 & 0 & 0 & 0 \\
0 & 0 & 0 & 0 & 0 & 0 & 0 & \times & \times & \times & 0 & 0 & 0 & 0 & 0 & 0 & 0 & 0 & 0 & 0 & 0 \\
0 & 0 & 0 & 0 & 0 & 0 & 0 & 0 & 0 & 0 & \times & \times & \times & 0 & 0 & 0 & 0 & 0 & 0 & 0 & 0 \\
0 & 0 & 0 & 0 & 0 & 0 & 0 & 0 & 0 & 0 & \times & \times & \times & 0 & 0 & 0 & 0 & 0 & 0 & 0 & 0 \\
0 & 0 & 0 & 0 & 0 & 0 & 0 & 0 & 0 & 0 & \times & \times & \times & 0 & 0 & 0 & 0 & 0 & 0 & 0 & 0 \\
0 & 0 & 0 & 0 & 0 & 0 & 0 & 0 & 0 & 0 & 0 & 0 & 0 & \times & \times & \times & \times & 0 & 0 & 0 & 0 \\
0 & 0 & 0 & 0 & 0 & 0 & 0 & 0 & 0 & 0 & 0 & 0 & 0 & \times & \times & \times & \times & 0 & 0 & 0 & 0 \\
0 & 0 & 0 & 0 & 0 & 0 & 0 & 0 & 0 & 0 & 0 & 0 & 0 & \times & \times & \times & \times & 0 & 0 & 0 & 0 \\
0 & 0 & 0 & 0 & 0 & 0 & 0 & 0 & 0 & 0 & 0 & 0 & 0 & \times & \times & \times & \times & 0 & 0 & 0 & 0 \\
0 & 0 & 0 & 0 & 0 & 0 & 0 & 0 & 0 & 0 & 0 & 0 & 0 & 0 & 0 & 0 & 0 & \times & \times & \times & \times \\
0 & 0 & 0 & 0 & 0 & 0 & 0 & 0 & 0 & 0 & 0 & 0 & 0 & 0 & 0 & 0 & 0 & \times & \times & \times & \times \\
0 & 0 & 0 & 0 & 0 & 0 & 0 & 0 & 0 & 0 & 0 & 0 & 0 & 0 & 0 & 0 & 0 & \times & \times & \times & \times \\
0 & 0 & 0 & 0 & 0 & 0 & 0 & 0 & 0 & 0 & 0 & 0 & 0 & 0 & 0 & 0 & 0 & \times & \times & \times & \times
\end{array}\right]. \quad (55)$$

The critical points A, B, C, and D, shown in Fig. 6(b), can be classified as the points where $\tilde{K}^{(-,+)}$, $\hat{K}^{(1)}$, $\hat{K}^{(2)}$, and $\tilde{K}^{(+,+)}$ respectively become singular. This means, in particular, that A and D are simple critical points and B and C are double critical points.

6.2 Search for bifurcation points

The original scaled corrector method and the revised one proposed in this paper were employed to search for the bifurcation points A, B, and C of the Hangai truss dome without resort to the eigenanalysis.

First, the original scaled corrector method was employed. The pseudo-eigenvalues $\hat{\lambda}$ for the scaled corrector $\mathbf{\Phi}^{\mathrm{sc}}$ in (17) were computed by (19) and plotted by ($\bullet$) in Fig. 7 against the vertical displacement of the center node. For comparison, the eigenvalues λ_i computed by the eigenanalysis are also shown in this figure by the dashed curves for simple eigenvalues and by the solid curves for double eigenvalues; both of these curves are monotone decreasing, and the zero crossing points of these curves correspond to the locations of those bifurcation points. The pseudo-eigenvalues plotted in this manner display a large scatter especially away from those bifurcation points. The zero crossing of the pseudo-eigenvalues $\hat{\lambda}$ indicated by ($\bullet$) is not very clear and it is difficult to determine the locations of bifurcation points.

Next, the revised scaled corrector method was employed. The pseudo-eigenvalues $\hat{\lambda}^{\mu}$ for $\mu = (+,+), (+,-), (-,+), (-,-), (1), (2)$ were computed by (30) and plotted in Fig. 8. Here, for $\mu = (1)$ and $\mu = (2)$, which are two-dimensional, two sets of $\hat{\lambda}^{\mu}$'s for $\mathbf{\Phi}^{(j)1}$ and $\mathbf{\Phi}^{(j)2}$ $(j = 1, 2)$ were computed by (51). It is noted that the corresponding diagonal blocks for $(+,-)$ and $(-,-)$ in (55) are one-dimensional and hence the pseudo-eigenvalues coincide exactly with the eigenvalues; accordingly, $\hat{\lambda}^{\mu}$'s for $(+,-)$ and $(-,-)$ display no

scatter. The pseudo-eigenvalues for μ other than $(+,-)$ and $(-,-)$ display scatters, which are significantly smaller than those for the original scaled corrector method in Fig. 7.

The zero crossing of the pseudo-eigenvalues $\hat{\lambda}^{\mu}$'s was recognized for

- $\mu = (-,+)$ corresponding to the bifurcation point A,
- $\mu = (2)$ to the bifurcation point B, and
- $\mu = (1)$ to the bifurcation point C.

From Table 1, the point A can be classified as a simple bifurcation point with D_3-invariant bifurcated path. The point B, at which pseudo-eigenvalues for $\mu = (2)$ cross zero, is a double bifurcation point with D_2^i-invariant $(i = 1, 2, 3)$ bifurcated paths. Likewise, the point C is a double bifurcation point with D_1^i-invariant $(i = 1, \ldots, 6)$ bifurcated paths. The multiplicity of bifurcation points has thus been identified by the revised method.

In addtion, we can see from Fig. 8 that the computed $\hat{\lambda}^{\mu}$'s serve as an upper bound on the true eigenvalue; it assesses the validity of (31).

6.3 Determination of bifurcation modes

For the simple bifurcation point A, the accuracy of the bifurcation mode $\mathbf{\Phi}^{\rm sc}$ computed by the scaled corrector method and that of $\mathbf{\Phi}^{(-,+)}$ by the revised method are compared with reference to the exact eigenvector $\mathbf{\Phi}_1$ for the smallest eigenvalue λ_1 computed by the eigenanalysis. We plot in Fig. 9 the values of $\cos\theta^{\rm sc} = (\mathbf{\Phi}^{\rm sc})^{\rm T}\mathbf{\Phi}_1$ and $\cos\theta^{(-,+)} = (\mathbf{\Phi}^{(-,+)})^{\rm T}\mathbf{\Phi}_1/||\mathbf{\Phi}^{(-,+)}||$, which should coincide with the unity when the computed bifurcation modes are exact. For the data of the scaled corrector method shown by the dotted line, the accuracy up to 5 digits is ensured only in a very close neighborhood of the bifurcation point A. For the data of the revised method shown by the solid line, such accuracy is ensured in a wide range of the abscissa, the center node displacement. This may suffice to demonstrate the superiority of the revised method.

For the double bifurcation point B, a pair of critical eigenvectors are to be obtained. The critical eigenvectors obtained by the scaled corrector method and the revised method are compared in Fig. 10. By the scaled corrector method, only a single bifurcation mode $\mathbf{\Phi}^{\rm sc}$, which does not necessarily coincide with the direction of a bifurcated path, was obtained at an equilibrium point. By contrast, by the revised method, two bifurcation modes $\mathbf{\Phi}^{(2)1}$ and $\mathbf{\Phi}^{(2)2}$ in (49) were successfully obtained; moreover, with the use of the bifurcation mode $\mathbf{\Phi}^{(2)1}$ obtained herein, bifurcated paths in the directions of (53) labeled by D_2^i $(i = 1, \ldots, 3)$ (cf., Table 1) can be found in a systematic manner.

For the double bifurcation point C, only a single bifurcation mode $\mathbf{\Phi}^{\rm sc}$ again was obtained by the scaled corrector method. By contrast, a pair of bifurcation modes $\mathbf{\Phi}^{(1)1}$ and $\mathbf{\Phi}^{(1)2}$ were successfully obtained by the revised method. Moreover, bifurcated paths in the directions of (52) labeled by D_1^i $(i = 1, \ldots, 6)$ can be found in a systematic manner.

As we have seen, the revised method is consistent with the bifurcation analysis at a double bifurcation point and, hence, is superior to the original scaled corrector method.

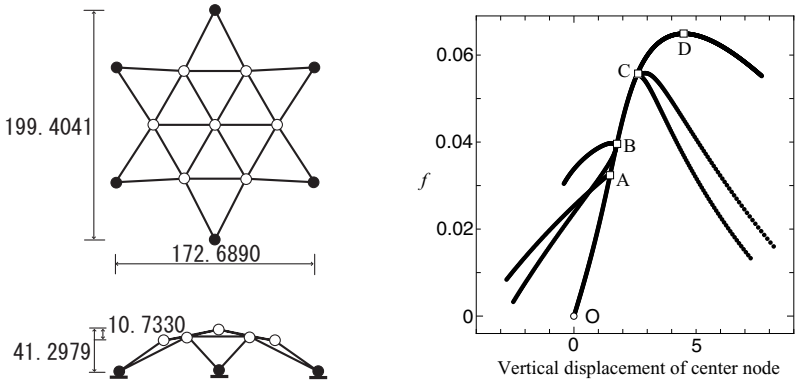

(a) Hangai truss dome (b) Curves of load versus displacement

Figure 6: The Hangai truss dome and its curves of load versus displacement

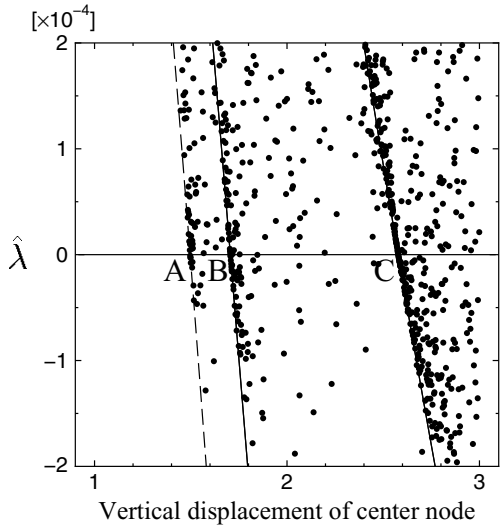

Figure 7: Pseudo-eigenvalue $\hat{\lambda}$ computed by the scaled corrector method for the Hangai truss dome (dashed and solid curves: simple and double eigenvalues λ_i computed by the eigenanalysis, respectively)

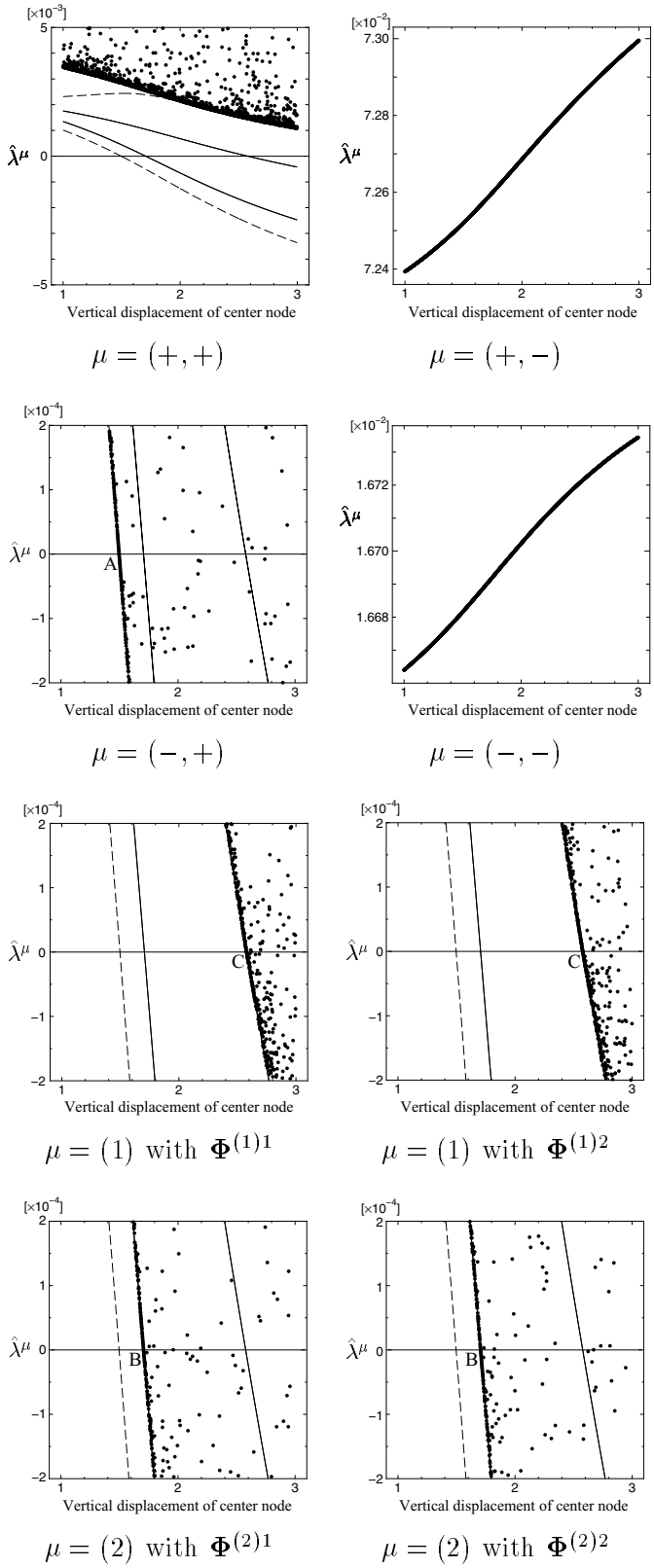

Figure 8: Pseudo-eigenvalue $\hat{\lambda}^\mu$ for each irreducible representation computed by the revised scaled corrector method for the Hangai truss dome (dashed and solid curves: simple and double eigenvalues λ_i computed by the eigenanalysis, respectively)

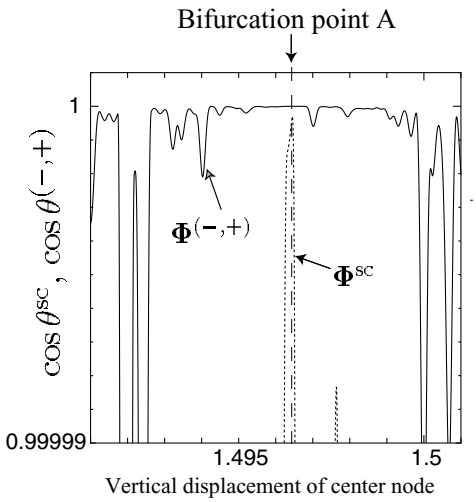

Figure 9: Comparison of the accuracy of the bifurcation modes $\Phi^{(-,+)}$ and Φ^{sc}

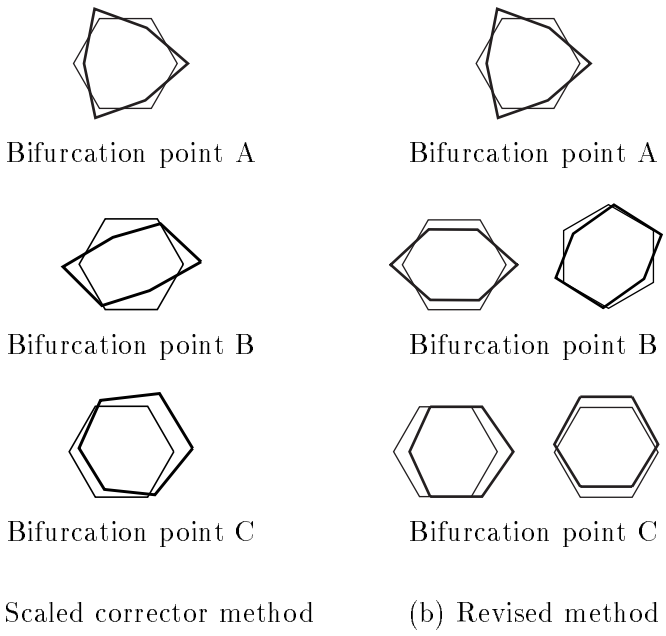

Figure 10: Critical eigenvectors for the Hangai dome expressed in terms of the plane view of the hexagonal nodes

7 Reticulated regular-hexagonal truss dome structure

As an example of a large-scaled symmetric structure, we refer to the regular hexagonal elastic reticulated truss dome structure with 50 layers shown in Fig. 11(a).

Finite displacement elastic bifurcation analysis was conducted to obtain the curves of load versus displacement shown in Fig. 11(b). All members of the dome are assumed to have the same cross section A and the same modulus of elasticity E; we set $EA = 1$ for normalization. The vertical load of cf was applied to the center node, the vertical loads of $2cf, 2^2cf, \ldots$ were applied to the 49 layers of the regular hexagonal nodes from inside towards outside, where $c = 6.28 \times 10^{-16}$ to normalize the loading pattern vector.

On the fundamental path with D_6-invariant deformation of this truss dome, there are four critical points:

- limit point E,
- bifurcation point F with D_1^i-invariant $(i = 1, \ldots, 6)$ bifurcated paths,
- bifurcation point G with D_2^i-invariant $(i = 1, 2, 3)$ bifurcated paths, and
- bifurcation point H with D_3-invariant bifurcated path.

Note that the critical points E and F are nearly coincidental.

7.1 Construction of the transformation matrix

The regular hexagonal truss dome structure shown in Fig. 11(a) consists of: one orbit of type 0 for the center node, 25 orbits of type 1V for hexagonal nodes, and 25 orbits of type 1M for hexagonal nodes in another direction. The transformation matrix H for this dome can be constructed through the assemblage of the column vectors for the orbits of types 0, 1V, and 1M shown in Fig. 5. The numbers of column vectors of H^μ, which represent the sizes of the blocks in (46), are listed in Table 2.

7.2 Search for bifurcation points

The original scaled corrector method and the revised one proposed in this paper were employed to search for the critical points E, F, G, and H of the regular-hexagonal truss dome without resort to the eigenanalysis.

First, the original scaled corrector method was employed to obtain the pseudo-eigenvalues $\hat{\lambda}$ plotted by $(\bullet)$ in Fig. 12. The zero crossing of the pseudo-eigenvalues can be clearly seen at the nearly coincidental critical points E and F; however, it is not possible to distinguish these points. It is difficult to locate the bifurcation points G and H.

Next, the revised scaled corrector method was employed to compute the pseudo-eigenvalues $\hat{\lambda}$ for $\mathbf{\Phi}^\mu$ in Fig. 13. Each of the four critical points E, F, G and H can be clearly recognized by the zero crossing of the pseudo-eigenvalues $\hat{\lambda}$'s for

- $\mu = (+, +)$ corresponding to the limit point E,
- $\mu = (1)$ to the double bifurcation point F,
- $\mu = (2)$ to the double bifurcation point G, and
- $\mu = (-, +)$ corresponding to the simple bifurcation point H.

The multiplicity of bifurcation points has thus been identified by the revised method. The bifurcation analysis can be conducted in a systematic manner with the use of the critical eigenvectors obtained by the proposed method.

Table 2: The numbers of column vectors of H^{μ} for the regular-hexagonal truss dome structure with 50 layers

Irreducible representation μ	Number of column vectors for H^{μ}
$(+,+)$	99
$(+,-)$	49
$(-,+)$	74
$(-,-)$	73
(1)	148+148
(2)	147+147

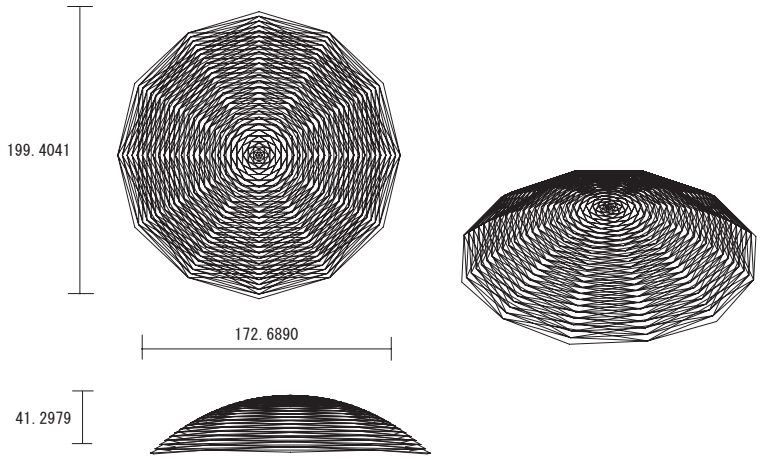

(a) Regular-hexagonal truss dome structure with 50 layers

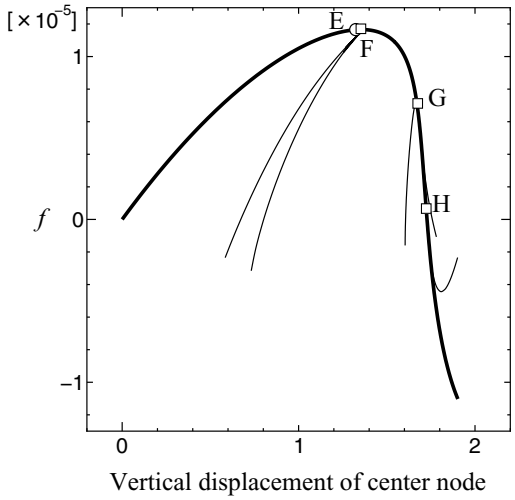

(b) Curves of load versus displacement

Figure 11: Reticulated regular-hexagonal truss dome structure and its curves of load versus displacement

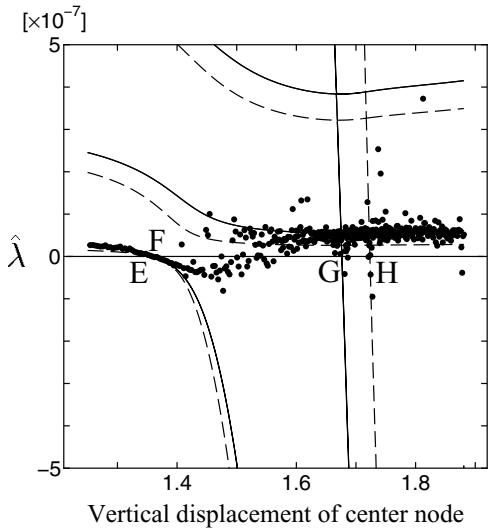

Figure 12: Pseudo-eigenvalue $\hat{\lambda}$ computed by the scaled corrector method for the reticulated regular-hexagonal truss dome (dashed and solid curves: simple and double eigenvalues λ_i computed by the eigenanalysis, respectively)

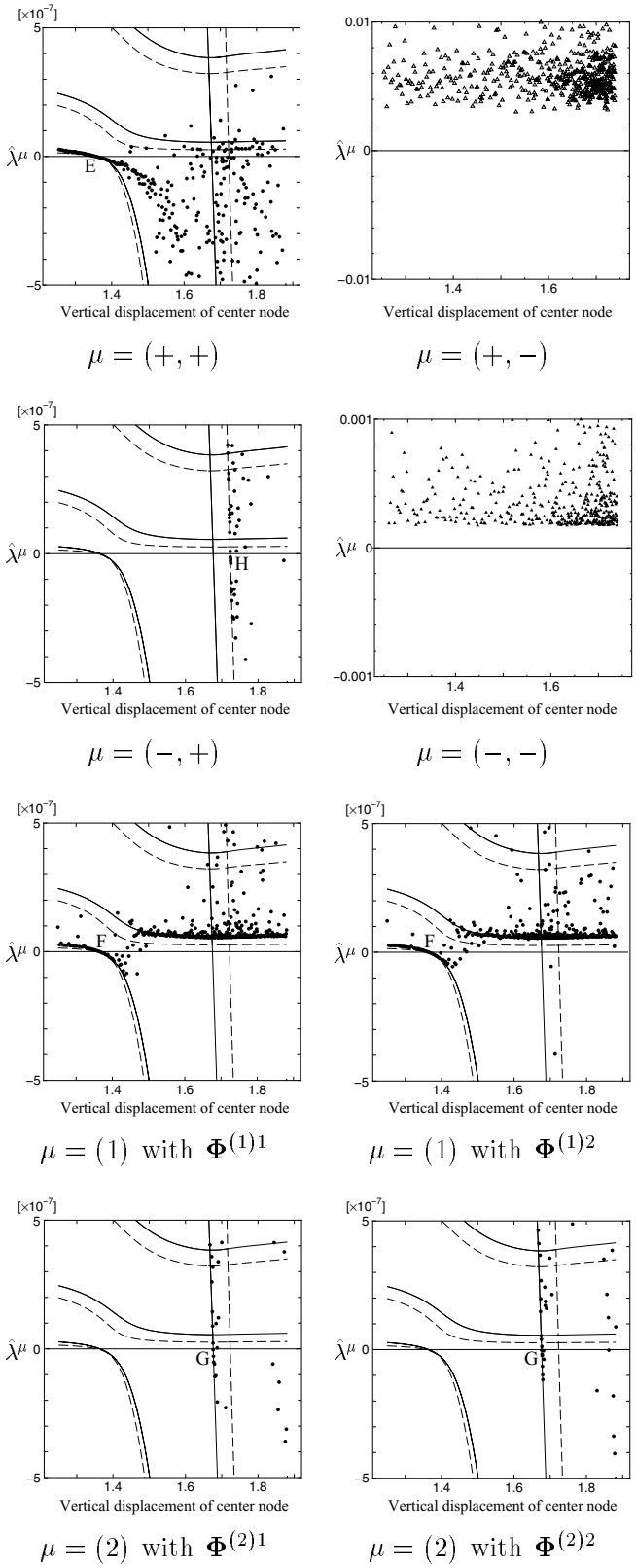

Figure 13: Pseudo-eigenvalue $\hat{\lambda}^\mu$ for each irreducible representation computed by the revised scaled corrector method for the regular-hexagonal truss dome with 50 layers (dashed and solid curves: simple and double eigenvalues λ_i computed by the eigenanalysis, respectively)

8 Conclusions

A new bifurcation analysis method that combines the mechanism of bifurcation of symmetric structure with the scaled corrector method is proposed. The method proposed is applied to the bifurcation analysis of reticulated regular-hexagonal truss domes to compute accurately the locations of double bifurcation points and nearly coincidental bifurcation points. Moreover, without resort to the eigenanalysis, a pair of critical eigenvectors at a double bifurcation point can be computed accurately and the bifurcated paths can be traced in a systematic manner. This shows the superiority of the proposed method over the original scaled corrector method.

References

[1] K.K. Choong, Y. Hangai, Review on methods of bifurcation analysis for geometrically nonlinear structures, Bulletin of the Int. Assoc. for Shell and Spatial Structures 34(2) (1993) 133–149.

[2] S. Dinkevich, Finite symmetric systems and their analysis, Int. J. Solids Struct. 27(10) (1991) 1215–1253.

[3] A. Eriksson, On some path-related measures for non-linear structural F. E. problems, Int. J. Numer. Methods Engrg. 26 (1988) 1791–1803.

[4] F. Fujii, K. Ikeda, H. Noguchi, S. Okazawa, Modified stiffness iteration to pinpoint multiple bifurcation points, Comput. Methods Appl. Mech. Engrg. 190(18-19) (2001) 2499–2522.

[5] F. Fujii, H. Noguchi, The buckling mode extracted from the LDL^T-decomposed large-order stiffness matrix, Commun. Numer. Methods Engrg. 18(7) (2002) 459–467.

[6] F. Fujii, E. Ramm, Computational bifurcation theory—path-tracing, pinpointing and path-switching, Engrg Struct. 19 (Links) (1997) 385–392.

[7] K. Gatermann, Computation of bifurcation graphs, in: E. Allgower, K. Georg, R. Miranda (Eds.), Exploiting Symmetry in Applied and Numerical Analysis, AMS Lectures in Appl. Math. 29, 1993, 187–201.

[8] K. Gatermann, B. Werner, Group theoretical mode interactions with different symmetries, Int. J. Bifurcation Chaos 4(1) (1994) 177–191.

[9] M. Golubitsky, I. Stewart, D.G. Schaeffer, Singularities and Groups in Bifurcation Theory, Vol. 2. Springer-Verlag, New York, 1988.

[10] T.J. Healey, A group theoretic approach to computational bifurcation problems with symmetry, Comput. Methods Appl. Mech. Engrg. 67(3) (1988) 257–295.

[11] T.J. Healey, J.A. Treacy, Exact block diagonalization of large eigenvalue problems for structures with symmetry, Int. J. Numer. Methods Engrg. 31(2) (1991) 265–285.

[12] K. Ikeda, I. Ario, K. Torii, Block-diagonalization analysis of symmetric plates, Int. J. Solids Struct. 29(22) (1992) 2779–2793.

[13] K. Ikeda, S. Murakami, I. Saiki, I. Sano, N. Oguma, Image simulation of uniform materials subjected to recursive bifurcation, Int. J. Engrg. Sci. 39(17) (2001) 1963–1999.

[14] K. Ikeda, K. Murota, Bifurcation analysis of symmetric structures using block-diagonalization, Comput. Methods Appl. Mech. Engrg. 86(2) (1991) 215–243.

[15] K. Ikeda, K. Murota, Imperfect Bifurcation in Structures and Materials: Engineering Use of Group-Theoretic Bifurcation Theory. Appl. Math. Sci. Ser. 149, Springer-Verlag, New York 2002.

[16] K. Ikeda, K. Murota, H. Fujii, Bifurcation hierarchy of symmetric structures, Int. J. Solids Struct. 27(12) (1991) 1551–1573.

[17] K. Ikeda, H. Sasaki, T. Ichimura, Diffuse mode bifurcation of soil causing vortex-like shear investigated by group-theoretic image analysis, J. Mech. Physics Solids 54(2) (2006) 310–339.

[18] F. Lin, Multi-solution theory of signal processing based on finite element method, Appl. Math. Comput. 161(1) (2005) 293–310.

[19] S.J. Mohan, R. Pratap, A group theoretic approach to the linear free vibrational analysis of shells with dihedral symmetry, J. Sound Vibration 252(2) (2002) 317–341.

[20] S.J. Mohan, R. Pratap, A natural classification of vibration modes of polygonal ducts based on group theoretic analysis, J. Sound Vibration 269(3–5), (2004) 745–764.

[21] K. Murota, K. Ikeda, Computational use of group theory in bifurcation analysis of symmetric structures, SIAM J. Sci. Statist. Comput. 12(2) (1991) 273–297.

[22] H. Noguchi, F. Fujii, Eigenvector-free indicator, pinpointing and branch-switching for bifurcation, Commun. Numer. Methods Engrg. 19(6) (2003) 445–457.

[23] H. Noguchi, T. Hisada, Development of a new branch-switching algorithm in nonlinear FEM using scaled corrector (in Japanese), Trans. Jap. Soc. Mech. Engrs, 58(555) (1992) 181–188 (2191–2198).

[24] M. Papadrakakis (Ed.), Solving Large-Scale Problems in Mechanics, the Development and Application of Computational Solution Methods. Wiley, Chichester, 1993.

[25] E. Riks, An incremental approach to the solution of snapping and buckling problems, Int. J. Soilds Struct. 15 (1979) 529–551.

[26] E. Riks, Some computational aspects of nonlinear structures, Comput. Methods Appl. Mech. Engrg. 47 (1984) 219–259.

[27] I. Saiki, K. Ikeda, K. Murota, Flower patterns appearing on a honeycomb structure and their bifurcation mechanism, Int. J. Bifurcation Chaos 15(2) (2005) 497–515.

[28] D.H. Sattinger, Group Theoretic Methods in Bifurcation Theory. Lecture Notes Math. 762, Springer-Verlag, Berlin, 1979.

[29] N.S. Sehmi, Large Order Structural Eigenanalysis Techniques, Algorithm for Finite Element Systems. Ellis Horwood, Chichester, 1989.

[30] R. Tanaka, I. Saiki, K. Ikeda, Group-theoretic bifurcation mechanism for pattern formation in three-dimensional uniform materials, Int. J. Bifurcation Chaos 12(12) (2002) 2767–2797.

[31] J.C. Wohlever, Some computational aspects of a group theoretic finite element approach to the buckling and postbuckling analyses of plates and shells-of-revolution, Comput. Methods Appl. Mech. Engrg. 170(3–4) (1999) 373–406.

[32] J.C. Wohlever, T.J. Healey, A group theoretic approach to the global bifurcation analysis of an axially compressed cylindrical shell, Comput. Methods Appl. Mech. Engrg. 122(3-4) (1995) 315–349.

[33] P. Wriggers, W. Wagner, C. Miehe, A quadratically convergent procedure for the calculation of stability points in finite element analysis, Comput. Methods Appl. Mech. Engrg. 70 (1988) 329–347.

[34] P.A. Wriggers, J.C. Simo, A general procedure for the direct computation of turning and bifurcation points, Int. J. Numer. Methods in Engng. 30 (1990) 155–176.

[35] A. Zingoni, A group-theoretic formulation for symmetric finite elements, Finite Elements Analysis Design 41(6) (2005) 615–635.

[36] G. Zloković, Group Theory and G-Vector Spaces in Structural Analysis. Ellis Horwood, Chichester, 1989.